Tunable Pulse-Shaping with Gated Graphene Nanoribbons

Ludmila Prokopeva[1], Naresh K. Emani[1], Alexandra Boltasseva[1,2], and Alexander Kildishev*,[1]
[1]*School of Electrical and Computer Engineering and Birck Nanotechnology Center, Purdue University, West Lafayette, IN 47907, USA*
[2]*DTU Fotonik, Department of Photonics Engineering, Technical University of Denmark, Lyngby, DK-2800, Denmark*
*Email: kildishev@purdue.edu**

Abstract: We propose a pulse-shaper made of gated graphene nanoribbons. Simulations demonstrate tunable control over the shapes of transmitted and reflected pulses using the gating bias. Initial fabrication and characterization of graphene elements is also discussed.
OCIS codes: (160.3918) Metamaterials; (160.4670) Optical Materials; (320.5540) Pulse Shaping

1. Introduction

Computer-controlled pulse-shaping continues to be an enabling technology for a broad range of important applications. For example, ultrafast pulse-shaping schemes are already being used for probing chemical processes, single molecules, or molecular systems where the methods of adaptive control are especially attractive to get a laser waveform producing the best experimental result defined by a given metric [1]. It would also be instrumental to have a compact, versatile, easy-to-control pulse-shaping device, which could be attached to the end of optical fiber or waveguide.

2. Geometry of the Pulse Shaper

For a proof-of-concept model of a tunable pulse shaping device we use a pair of graphene nanoribbons (25-nm wide, 25-nm spaced) as controllable dispersive elements. The nannoribbons are separated by a 20-nm thick dielectric spacer ($\varepsilon_2 = 2.25$), and the structure is placed on a substrate ($\varepsilon_3 = \varepsilon_2$), as shown in fig. 1a, $\varepsilon_1 = 1$.

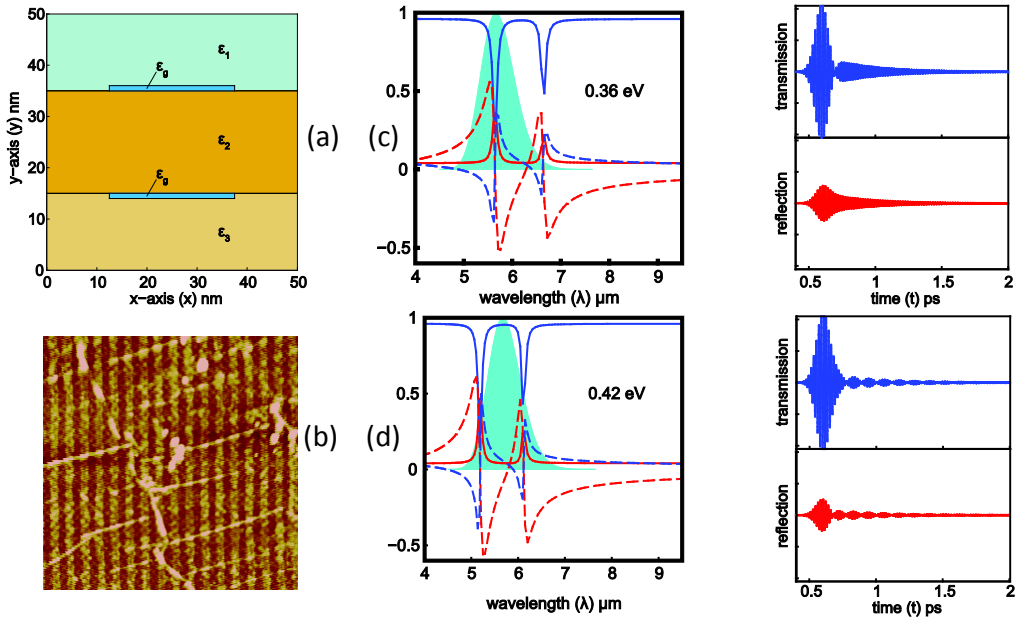

Figure 1 (a) Schematics of a pulse shaping device; (b) Atomic Force Micrograph of fabricated graphene nanoribbons; (c-d) Device spectrum (left) and the pulse shapes (right) simulated for two chemical potentials of the graphene elements, $E_F = 0.36$ eV and $E_F = 0.42$ eV; solid lines, red and blue, show reflectance and transmittance, dashed lines; red and blue, show phase of reflection and transmission.

3. Numerical Modeling

The structure exhibits resonances in the near IR to mid IR spectral ranges. The strength and spectral locations of resonances depend on the carrier concentration in the nanoribbons, which can be electrically controlled by an applied gate voltage. In this way, resonances can be moved in or moved out, hence causing no interaction with the spectrum of the incident pulse (shown as area plot in figs. 1c and 1d, left panels). It is the presence of tunable, close-

ly positioned sharp resonances with phase jumps in the spectra that allows for obtaining substantially different pulse shapes of the transmitted and reflected pulses vs. the gating bias, as shown in figs. 1c and 1d (right panels).

For our preliminary proof-of-concept modeling, we use random phase approximation expressions to model the surface conductivity (σ_s) of graphene elements [2]. We assume room temperature and tunable chemical potential E_F in the range 0.1-0.6 eV. We take a realistic scattering rate (yet to be fitted with optical characterization of our experimental samples) $\Gamma = \hbar v_F^2 \,/\, (\mu \mathrm{E}_F)$ being a function of DC mobility $\mu = 1\,[\mathrm{m^2V^{-1}s^{-1}}]$ and chemical potential E_F, e.g. [3]. Using the above assumptions, we have used a semi-analytical Spatial Harmonic Analysis (SHA) method [4, 5], where small effective thickness and volume permittivity have been introduced for graphene elements, $\delta = 0.01\ \mathrm{nm}$ and $\varepsilon_g = 1 + \iota\sigma_s\varepsilon_0^{-1}\hbar\omega^{-1}\delta^{-1}$. A larger effective thickness (e.g. $\delta = 1\ \mathrm{nm}$ is usually enough for convergence for a single whole layer graphene) results in noticeable red shift of the spectrum. Specifically, figs. 1c and 1d show the shapes of the transmitted and reflected pulses simulated by SHA and FFT-ed for a Gaussian incident pulse (width $\sigma = 60\,\mathrm{fs}$, carrier $\lambda_c = 5.6653\,\mu\mathrm{m}$). For $E_F = 0.42\,\mathrm{eV}$ (fig. 1d) both resonances are within the incident spectrum, and the pulse transforms to a sequence of pulses once transmitted or reflected from the device. For $E_F = 0.36\,\mathrm{eV}$ (fig. 1c) the pulse center coincides with one resonance and another resonance is off the incident spectrum, the pulse then splits into two. A similar effect is observed for another resonance with $E_F = 0.49\,\mathrm{eV}$ (not shown). Moving both resonances away from overlapping with the incident spectrum restores the initial Gaussian profile of the incident pulse.

4. Fabrication Method

We have successfully fabricated initial samples of graphene nanoribbons using commercially available single layer CVD graphene on oxidized silicon substrates (Graphene Laboratories Inc). This was achieved by patterning of 50 nm thick e-beam resist (PMMA) and subsequent dry etching using oxygen plasma. A representative atomic force micrograph of the fabricated sample is shown in fig. 1b. In the near future we plan to characterize these samples to validate the numerical model used in our simulations.

5. Conclusion

We proposed a tunable pulse-shaper consisting of a gated pair of graphene nanoribbons. The initial simulations confirm a desired pulse shaping capability. We have shown the initial fabrication of graphene nanoribbons, and the experimental validation of the proposed device is underway.

Our numerical studies show that when dealing with structured graphene, the volume-based numerical approach used here is optimal neither for semi-analytical mode-matching methods (large number of modes may be required), nor for mesh-based methods like FDTD (small thickness requires either extremely fine grid or using sub-gridding). Instead, surface current should be introduced as a boundary condition replacing continuity of tangential magnetic field. We have already extended our SHA solver for low-dimensional material elements (like graphene). Also accurate full-wave time domain modeling of graphene, including interband and intraband contributions, is available by combining critical-point approach [6] with surface-current enabled FDTD scheme [7]. The latter will be published in detail elsewhere.

Authors acknowledge support from grants: ARO MURI 56154-PH-MUR (W911NF-09-1-0539) and ARO 63133-PH (W911NF-13-1-0226).

6. References

[1] A. M. Weiner, "Ultrafast optical pulse shaping: A tutorial review," Opt. Commun. **284**, 3669-3692 (2011).
[2] L. Falkovsky, "Optical Properties of Graphene," J. Phys.: Conf. Ser. **129**, 012004 (2008).
[3] J. Christensen, A. Manjavacas, S. Thongrattanasiri, F. H. L. Koppens, and F. J. Garcia de Abajo, "Graphene Plasmon Waveguiding and Hybridization in Individual and Paired Nanoribbons," ACS Nano **6**, 431–440 (2011).
[4] X. Ni, Z. Liu, F. Gu, M. G. Pacheco, J. Borneman, and A. V. Kildishev, "PhotonicsSHA-2D: Modeling of Single-Period Multilayer Optical Gratings and Metamaterials," DOI: 10.4231/D3WS8HK4X (2012).
[5] Z. Liu, K.-P. Chen, X. Ni, V. P. Drachev, V. M. Shalaev, and A. V. Kildishev, "Experimental verification of two-dimensional spatial harmonic analysis at oblique light incidence," J. Opt. Soc. Am. B **27**, 2465-2470 (2010).
[6] L. J. Prokopeva, A. V. Kildishev, "Efficient time-domain model of the graphene dielectric function," Proc. SPIE 8806, Metamaterials: Fundamentals and Applications VI, 88060H (September 11, 2013); doi:10.1117/12.2024205.
[7] V. Nayyeri, M. Soleimani, and O. M. Ramahi, "Modeling Graphene in the Finite-Difference Time-Domain Method using a Surface Boundary Condition," IEEE Trans. Antennas Propag. **61**, 4176-4182 (2013).